First-principles simulations of PVDF copolymers with high dielectric energy density: PVDF-HFP and PVDF-BTFE

Rui Dong, V. Ranjan, Marco Buongiorno Nardelli, and J. Bernholc

First Principles Simulations of PVDF Copolymers With High Dielectric Energy Density: PVDF-HFP and PVDF-BTFE

Rui Dong,[1] V. Ranjan,[1] Marco Buongiorno Nardelli,[1,2] and J. Bernholc[1]

[1]*Department of Physics, North Carolina State University, Raleigh, NC, 27695, USA*

[2]*Department of Physics and Department of Chemistry, University of North Texas, Denton, TX 76203,*

USA

Phase diagrams of polyvinylidene fluoride (PVDF) and its copolymers with hexafluoropropylene (HFP) and bromotrifluoroethylene (BTFE) are investigated via first-principles simulations and compared to previously studied P(VDF-chlorotrifluoroethylene) (CTFE) data. We find that a non-polar to polar phase transition induced by an electric field also occurs in HFP and BTFE copolymers and the results for P(VDF-HFP) show good agreement with existing experiments. For P(VDF-BTFE), we show that its non-polar phase remains the ground state for a substantially larger range of concentrations than for P(VDF-CTFE) and P(VDF-HFP), and predict that a high BTFE concentration copolymer will achieve a significantly higher energy density at low field than P(VDF-CTFE) 9%. The transition pathways connecting the polar and non-polar phases are also calculated and the energy barriers for the transitions turn out to be similar for the three copolymers, even at different co-monomer concentrations. The similarity of barriers indicates that a mixture of these and related copolymers can be used to optimize the properties of the dielectric, such as energy density, processability, and cost.

I. INTRODUCTION

Polyvinylidene fluoride (VDF) is a well-established fluoropolymer known for its toughness and chemical stability. It is used in a variety of applications taking advantage of its thermoplasticity, structural and chemical resilience, and insulating properties. More recently, however, the ferroelectric properties of PVDF family, defined as P(VDF-co-monomer), with co-monomers being other similar units, such as trifluoroethylene (TrFE) or chlorotrifluoroethylene (CTFE), attracted significant attention because they can form relaxor ferroelectrics with much increased capacitive energy density [1] and high efficiency electrocaloric materials[2]. The PVDF chain has a large spontaneous polarization that originates from the charge distribution in the VDF (CF_2-CH_2) repeat unit[3–5]. PVDF can form several different crystal phases with zero, moderate and large polarization. Calculations show that the zero polarization phase has the lowest energy[6]. However, in a large electric field the polar dipoles will align with the field, lowering the enthalpies of the polar phases, potentially leading to phase transitions that could be used to store energy. However, pure PVDF is not suitable for energy storage, because the strong coupling between its chains hinders molecular realignment with the electric field and inhibits crystallization. It also leads to a large remanent polarization and causes loss. Studies show that admixture of co-monomers such as TrFE or tetrafluoroethylene (TeFE) dramatically increases crystallinity and reduces the coupling between dipoles[7]. Adding a large third monomer to form a terpolymer system[8] or irradiating to form chemical pinning[9,10] further reduces ferroelectric coupling between domains.

One of the principal potential applications of ferroelectric polymers is as dielectrics in capacitors, in which they could store substantial amounts of energy while allowing for rapid discharge. The current state-of-the-art dielectric material is bi-axially oriented polypropylene (BOPP). However, its energy density is only 4 J/cm^3. In 2006, a blend of PVDF with 9% CTFE

was found to have ultrahigh energy density of more than 18 J/cm^3[1], and in 2009 PVDF[11] with 4.5% hexafluoropropylene (HFP) was found to have similar performance. In these copolymer systems, the dielectric displacement $\vec{D}$ increases non-linearly with the electric field $\vec{E}$. The non-linear behavior is the reason for the ultrahigh energy density, with late saturation of $\vec{D}$ and high breakdown field both being essential.

PVDF copolymers exist in both non-polar and polar phases, and we have previously shown that a non-polar to polar phase transition in P(VDF-CTFE) polymers is responsible for the ultrahigh energy density[6]. Our results indicate that P(VDF-CTFE) copolymers with CTFE concentration below 30% have a non-polar ground state. Since a polar phase has lower electric enthalpy in high enough electric field, a transition to the polar state will eventually occur as the field is increased. However, the observed increase in dielectric displacement is gradual rather than abrupt. Ref. [6] thus assumed that the experimental sample consists of nano domains with different CTFE concentrations, which give the overall measured concentration (e.g. 9% of CTFE in Ref[1]). As the field increases, different domains convert to the polar phase as their critical field is reached. This leads to the observed non-linear increase in dielectric displacement and the ultrahigh energy density.

We have subsequently investigated the mechanism of the non-polar to polar transition and uncovered a two-step transition pathway connecting the two phases. The two-step rotational and torsional pathway has a calculated activation barrier of 100 meV/carbon atom in pure PVDF. In a material with 10% CTFE, the calculated barrier is 70 meV/carbon atom, which makes the transition easier to be triggered by thermal fluctuation. This barrier is further reduced in the presence of an electric field, because the intermediate stages have significant polarizations that lower their enthalpies. In the current work, we first investigate P(VDF-HFP) copolymers and

show that the larger size of HFP results in two times greater effectiveness in enhancing electric-field-induced energy storage than CTFE, in nearly perfect agreement with experiment. We then investigate PVDF-bromotrifluoroethylene (BTFE) copolymers and predict that P(VDF-BTFE) could be a very good candidate for a high power density dielectric requiring much lower field strengths than either P(VDF-CTFE) 9% or P(VDF-HFP) 4.5%. In general, the similarities of the phase diagrams and transformation pathways for the three copolymer systems provide an opportunity to use their combinations to optimize not only the dielectric properties, but also cost and processability.

The rest of this paper is organized as follows: Section II describes the methodology and calculations, while Sections III and IV provide results for P(VDF-HFP) and P(VDF-BTFE), respectively, discussing their phase transformations as a function of the electric field, dielectric properties, and field-induced structural transition pathways. Our Summary and Conclusions are presented in Section V.
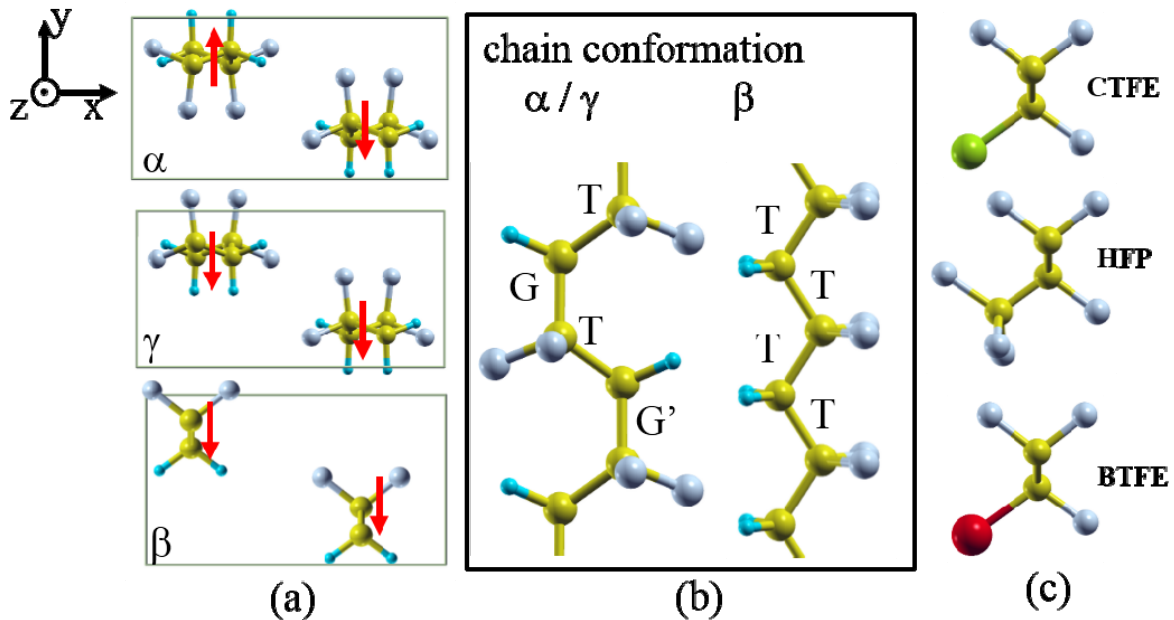
FIG. 1. Geometries of three crystal phases of PVDF and the three copolymer units discussed here: (a) Polymer chain arrangements in the α, β and γ phases of PVDF. (b) Conformations of the carbon backbone: TGTG' in the α and γ phases and all T in the beta β phase, where T and G denote *Trans* and *Gauche* bond arrangements, respectively. (c) Three co-monomer units, from the top: CTFE, HFP, BTFE. Color code: carbon - yellow, hydrogen - light blue, fluorine - grey, chlorine - green, bromine - red.

II. METHODOLOGY AND CALCULATIONS

A. STRUCTURES, PHASE EQUILIBRA AND ENERGY DENSITY

PVDF exists in several possible crystalline phases[12] and three of them, shown in Fig. 1(a), are involved in the non-polar to polar phase transition. The α phase has the TGTG' chain conformation in which the dihedral angles of the carbon backbone alternate between 60° and 180°. Each TGTG' chain has a weak dipole moment, as indicated by the arrows in the top panel of Fig. 1(a), but the antiparallel packing cancels the net polarization in the unit cell. The primitive cell of the α phase has space group of C_{2h}^5. The γ phase is formed by the same TGTG' chains but with parallel packing, see the middle panel in Fig. 1(a). The primitive cell of the γ phase has space group of C_{2v}^9. It has a moderate dipole moment per unit cell. In the β phase (space group C_{2v}^{14}), the carbon chains have an all *Trans* configuration and all the dihedral angles equal to 180°. Close-ups of TGTG' and all *Trans* chains are shown in Fig. 1(b). In the β phase the dipoles are significantly larger and they are all aligned. Therefore, it has much stronger polarization than the γ phase.

The structures of CTFE (CF$_2$-CFCl), HFP (CF$_2$-CF-CF$_3$) and BTFE (CF$_2$-CFBr) co-monomers considered in this paper are displayed in Fig. 1 (c). Experiments[8] show that the copolymer systems also form crystal phases with TGTG' and all-trans chains, but there are no

5

crystallographic measurements of their structures. The supplementary information provides atomic coordinates of several of these structures.[13]

For the pure PVDF and P(VDF-CTFE) with low CTFE concentration, the non-polar α phase has the lowest energy according to density-functional calculations [6]. However, the polar β phase can be stabilized in a large electric field by lowering the electric enthalpy $H(\vec{E})$,

$$H(\vec{E}) = U - \Omega \vec{P} \cdot \vec{E}, \tag{1}$$

where U is the internal energy, approximated here as the total energy in density-functional-theory calculations, Ω is the volume, and $\vec{P}$ and $\vec{E}$ are polarization and electric field, respectively. In experiments, PVDF copolymers are made into thin films in which the chains are parallel to the film and the electric field is applied perpendicular to the film. After the first poling cycle in which a large electric field is applied, all effective dipoles are aligned with the direction of the electric field. Therefore, we only consider the electric field along the y-axis in this work, see Fig. 1(a). Under a high enough electric field, the β phase will have lower enthalpy than the α phase and a phase transition will occur. The critical field for the onset of the transition is

$$E_c = \frac{U_\alpha - U_\beta}{\Omega P}. \tag{2}$$

In experiments [1], the increase in displacement field $\vec{D}$ with an increasing electric field is gradual rather than abrupt, which results in the desired gradual increase in the stored energy. The gradual increase can be explained by the well-known fact that a relaxor ferroelectric, such as a PVDF-copolymer mixture, consists of nanoscale domains[10]. Ref. [6] thus assumed that the copolymer concentration in the various nano domains is not uniform throughout the material. Each domain has its own co-monomer concentration and thus a corresponding value of the critical field. When

$\vec{E}$ reaches the critical value for one particular concentration, all domains with this concentration can thus convert from the non-polar to the polar phase. Since this is a first order transition (see below), an activation energy needs to be thermally overcome, but small activation energies in nano domains can lead to fast kinetics. Following Ref.[6] we assume a Gaussian broadening of the concentration

$$n(x) = C \cdot Exp(-\frac{(x-x_0)^2}{2\sigma^2}), \tag{3}$$

where x is the concentration, σ is the broadening width, and C is the normalization factor. Ref.[6] was able to reproduce the experimental data for P(VDF-CTFE) well by using the broadening as a single fitting parameter.

Assuming fast kinetics, when a critical field of a certain domain is reached, it converts to the polar phase. The gained polarization is accumulated in the total dielectric displacement D. After D vs. E relation is obtained, the energy density is calculated using

$$\xi = \int_0^{D_{max}} E(D) \, dD. \tag{4}$$

Even with a broadening in the range of a few percent, the nano domain model leads to a wide gamut of critical fields. The sample is thus able to respond to a large range of electric fields. This is the reason for the nonlinear increase of dielectric displacement and the experimentally observed very late saturation with increasing electric field.

Turning to structural modeling, we use supercells containing two PVDF chains for all three phases. To get different co-monomer concentrations, supercells with various backbone lengths are chosen and one VDF unit of each chain is replaced by a co-monomer. Sample PDB files are provided in supplementary material. In this approach, only a few values of concentration can be

modeled, and the quantities $\Delta U_{\alpha-\beta}$, P and E_c for other concentrations are obtained by interpolation. We tested placing the co-monomer units at various places in the polymer backbone, but these different "doping" models have comparable total energies. In the test case of 12.5% PVDF-CTFE, we calculated all five possible doping models, which give average $\Delta U_{\alpha-\beta}$ of 15.22 meV/carbon atom and variation of 2.94 meV/carbon atom. We thus use the same doping positions for consistency.

B. TRANSFORMATION PATHWAY

Ref. [14] uncovered a low-energy transformation pathway directly connecting the non-polar α phase and the polar β phase. Since the PVDF chains are strongly bonded, a low energy path cannot involve bond breaking and only bond, angle, and chain rotations should be involved. Furthermore, a direct switch of one monomer from gauche to trans configuration involves an energy change of ~1 eV, which is too costly[5]. Ref.[14] considered a series of concerted transformations, which turn out to have much lower barriers. The pathway is schematically shown in Fig. 2 and involves two steps. In the first step, the non-polar α phase, which has a unit cell with two chains of opposite polarizations, transforms into the polar γ phase by rotating a chain to align its dipole moment with that of the other chain. Defining the interchain angle θ as the angle between the dipole moments, the α phase corresponds to θ = 180° and the γ phase to θ = 0°. While the γ phase only has a moderate polarization, its dipoles are already aligned, which facilitates the transformation to the β phase. The latter step requires changing the TGTG' chains to all T. Denoting the dihedral angle as φ, in the TGTG' chain the dihedral angles alternate between two values: 60° and 180°. Gradually changing the φ = 60° angles to 180° constitutes the second part of the transformation pathway, resulting in a β-phase crystal.

As will be shown below, both transformations have activation barriers, and therefore need to rely on thermal fluctuations to proceed. However, according to Eq. (1), an applied electric field will lower the electric enthalpies along the entire pathway, except at the starting point, the non-polar α phase. To calculate the electric enthalpies along the transformation pathway we use a "rigid dipole" approximation, assuming that the dipole moment of the VDF monomer is fixed and that the different values of polarization along the pathway come from the orientations of VDF units, and thus the total polarization can be calculated from interchain and dihedral angles. This approximation was previously tested and found to reproduce Berry phase calculations within a few percent [14].

Since the transformations are activated, we must show that the activation barriers are small enough for the transformations to occur quickly enough at room temperature to be practical for energy storage. This is indeed the case for all the copolymer mixtures discussed here. In fact, their activation barriers turned out to be very similar (see Section III).
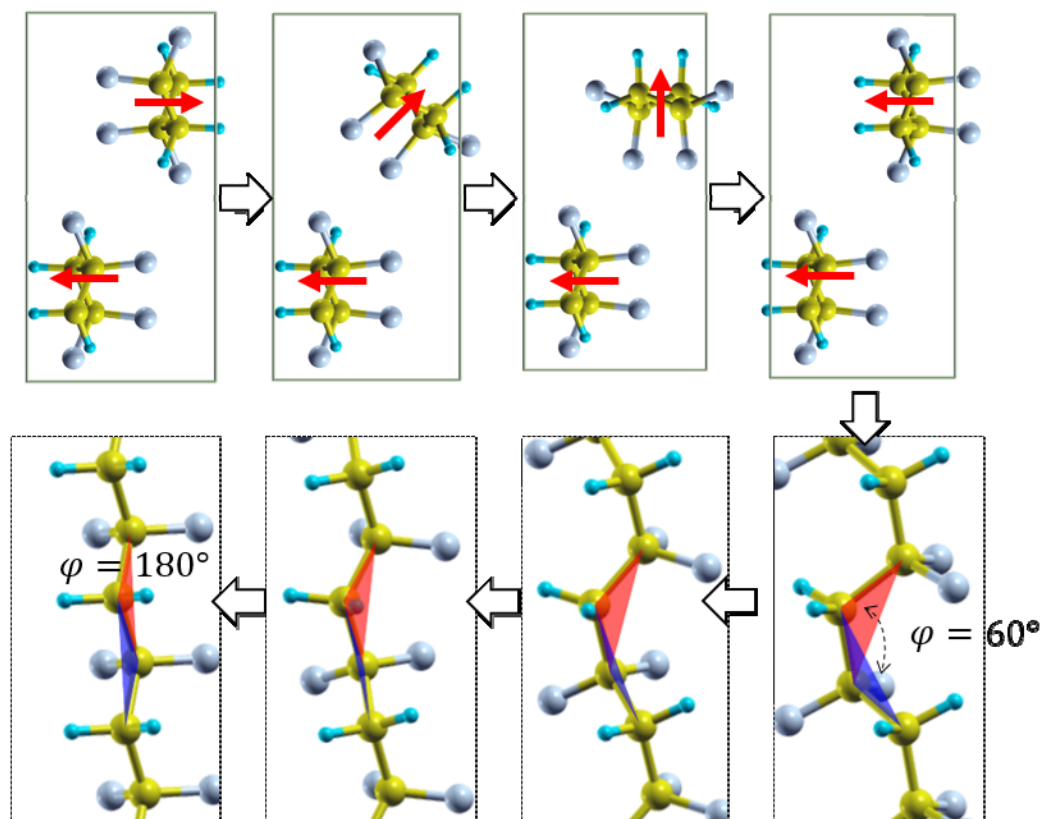
FIG. 2. The two-step transition pathway connecting the non-polar α phase and the polar γ and β phases. The top panels show the conversion to the γ phase through a rotation of one chain. The bottom panel illustrates dihedral angle changes in the TGTG' chain as it transforms to the all T chain of the β phase. Red arrows indicate the directions of the dipole moments while black double arrows indicate the geometrical progression, see text.

C. CALCULATIONS

All calculations are carried out within the framework of Density Functional Theory (DFT), using the plane wave package QuantumEspresso (QE)[15]. We use 50 and 600 Rydberg (Ry) cutoffs for the wave functions and charge density, respectively. These values are much higher than in normal calculations using ultrasoft pseudopotentials[16]. This is because our convergence tests show that the potential energy surface of PVDF-based polymers is extremely flat, and very high

energy cutoffs are needed to converge the geometry. Reciprocal space sampling does not play as important a role in the convergence as the energy cutoff; 2x4x4 Monkhorst-Pack k-point grid[17] is chosen for the primitive α-PVDF unit cell and is modified accordingly for larger cells. Since dipole-dipole interaction dominates the interchain binding in PVDF-based polymers, our tests using the vdW-DF functional[18] and the DFT+D method[19] do not show a systematic improvement in structural parameters over the simpler PBE[20] functional. Therefore, the PBE exchange-correlation functional is used throughout the current work.

The cell parameters and the atomic positions are relaxed via BFGS optimization procedure [21] until all force components are smaller than 0.01 eV/Å^3 and all stress components are smaller than 0.5 KBar. We choose such restrictive convergence criteria for the same reason – the potential energy surface is extremely flat. Berry phase calculations[22] are then carried out for the optimized end structures to obtain the polarization.

III. RESULTS AND DISCUSSION

In this Section we describe and discuss in separate subsections the results for P(VDF-HFP) and P(VDF-BTFE). In the first case, experimental data already exist and the results are used to understand and explain the data. For P(VDF-BTFE) the results constitute a prediction, to be explored and validated by experiments.

A. P(VDF-HFP)
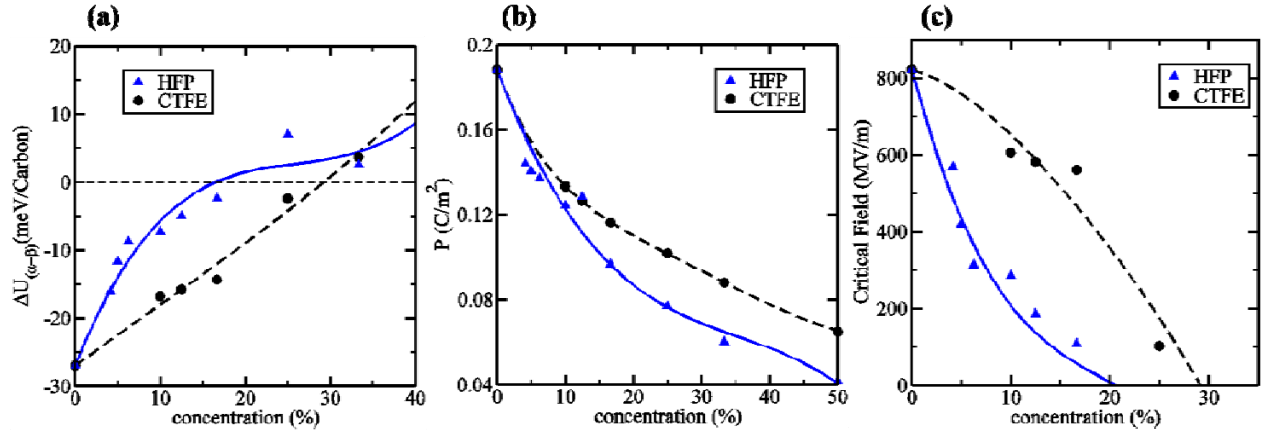
FIG. 3. Phase equilibria and dielectric properties of P(VDF-HFP) copolymers vs. concentration, with P(VDF-CTFE) data also shown as a benchmark. (a) Energy difference between α and β phases (negative value means that the α phase is more stable), (b) Polarization. (c) Critical field at the phase transition.

Zhang's group has shown that the P(VDF-HFP) 4.5% copolymer reaches the breakdown field of more than 700 MV/m and energy density of more than 25 J/cm^3 [11] . The 4.5% HFE copolymer has thus very similar energy density to P(VDF-CTFE) 9%[1]. Based on the methodology described above, we calculate the total energy of α and β phases of P(VDF-HFP) copolymers with varying concentrations. Due to the limited size of computationally tractable supercells, we cannot carry out calculations for arbitrary concentrations and can only consider certain values. For example, we use 10% concentration to mimic 9% copolymer sample, and 4.17% for 4.5%. The curves shown in Fig. 3 are polynomial interpolations between the computed values. The total energy difference $\Delta U_{\alpha-\beta}$ vs. concentration is plotted in Fig. 3(a), with previously calculated data for P(VDF-CTFE) as a benchmark. The energy difference ΔU determines the relative stability of the two phases, with a negative value indicating that the α phase is more stable. The HFP co-monomer unit is much larger than CTFE and it leads to a much greater change in geometry,

resulting in a distinct energy difference curve. As a function of concentration, ΔU increases sharply to zero at about 17%. The corresponding phase equilibrium is reached at about 30% for P(VDF-CTFE). As a consequence, $|\Delta U|$ is much smaller for P(VDF-HFP) at the same concentration (when $\Delta U < 0$). Although the polar phase is more preferred in P(VDF-HFP) from the energy diagram, both systems behave in essentially the same fashion and the phase transition mechanism is available in the appropriate concentration region. In our simulations, the energy differences between the phases are close for the two cells with 10% CTFE and 4.17% HFP. Fig. 3(b) shows the polarizations of the two copolymers, and they decrease as the concentration increases for both systems. The reasons are twofold: (i) the co-monomer unit has nearly zero dipole moment and higher co-monomer concentration leads to a larger fraction of non-polar units; (ii) a larger co-monomer unit expands the cell and therefore reduces the polarization. P(VDF-HFP) has a significantly larger unit cell volume, and consequently a smaller polarization at the same concentration. The critical field E_c is calculated using Eq. (2) and plotted in Fig. 3(c). The 4.17% HFP and 10% CTFE cells also have very similar critical fields, i.e., they will be converted to polar phases at similar electric fields.
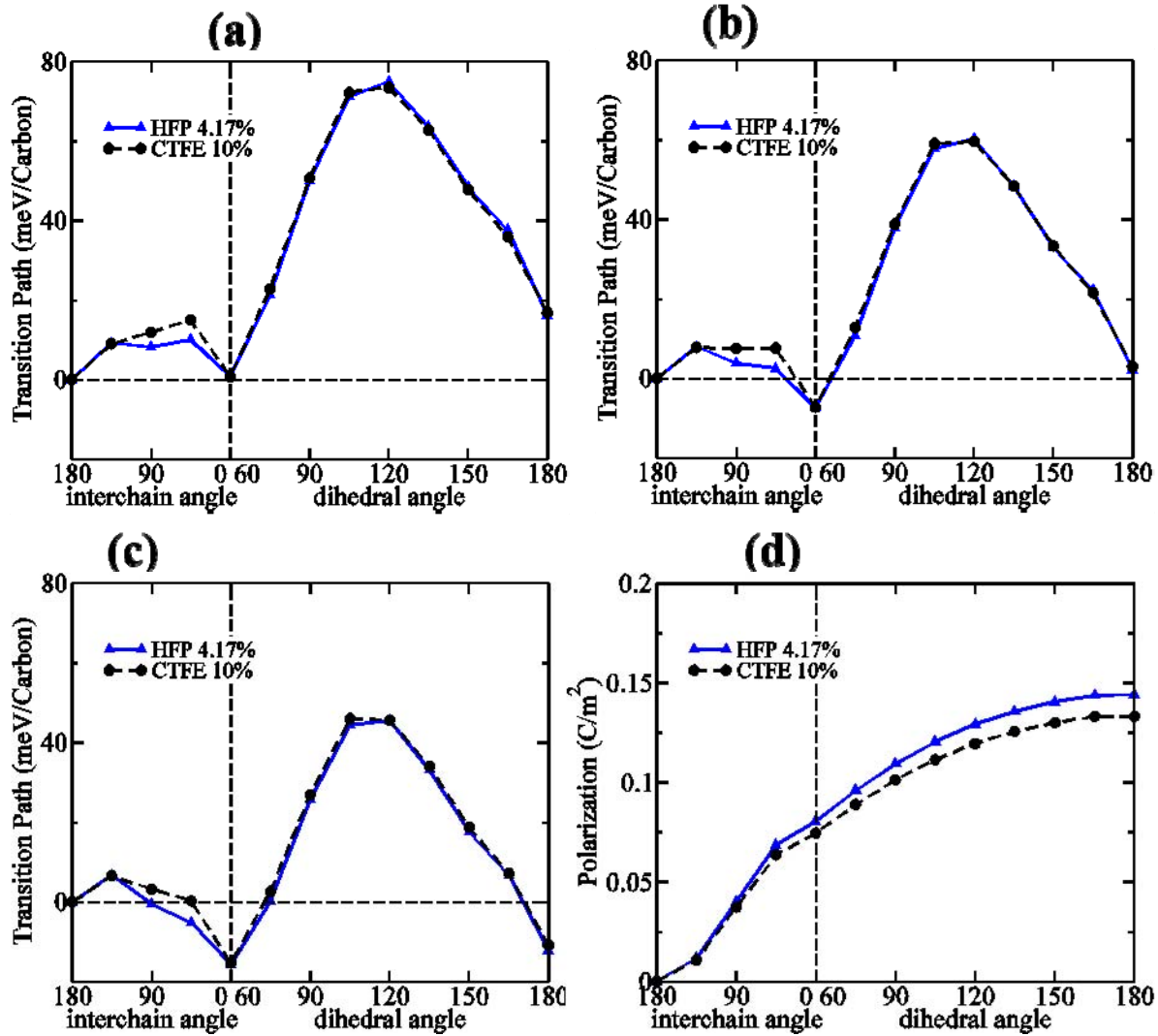
FIG. 4. Total energy along the transition pathway from the α phase to the β phase for P(VDF-HFP) 4.17%, with data for P(VDF-CTFE) 10% also shown for comparison: (a) at zero electric field, (b) at 500 MV/m, (c) at 1000 MV/m. (d) Polarization along the pathway. The total energy of the α phase is used as reference and is set to 0. The vertical dashed line divides the transition path into two parts: α → γ and γ → β. The angles are defined in Fig. 2.

The α to β transition pathway of 4.17% HFP is displayed in Fig. 4, together with benchmark results for 10% CTFE. Panels 4(a)-(c) show the energy pathways in 0, 500, and 1000 MV/m electric fields, respectively, and panel 4(d) plots polarization along the path. The two copolymers

again exhibit almost identical properties along the path. Note that there are energy barriers for both steps and the barrier in the second step is dominant. It is 100 meV/carbon in pure PVDF. However, admixture of 4.17% HFP or 10% CTFE reduces the barrier to 70 meV/carbon atom without electric field, and 50 meV/carbon atom at the very high field of 1000 MV/m. The closeness of our results for the 4.17% HFP and 10% CFTE for both phase equilibria and transformation pathways is in excellent agreement with experimental measurements of dielectric performance [1],[11] and shows that our methodology and conceptual model describe well the dielectric properties of PVDF copolymers.

We should stress that the above model does not consider the kinetics of the transformation or the morphology of the film. It is well-known that PVDF-based polymer films consist of nanoscale domains, both polycrystalline and amorphous [3]. The cooperative mechanism described above would lead to flipping of a few monomer units at a time, due to kinetic constraints. Since 1/3 of the atoms are carbon and the largest barriers are ~70 meV/carbon atom, thermal fluctuations at room temperature are certainly sufficient to enable the above transformations. Since the volumes of the two phases differ, the phase transition is first order and the new phase must form nuclei of sufficient sizes for the phase transition to occur. While the kinetics of this process cannot be studied by ab initio methods at present and thus is beyond the scope of the paper, the experimental and theoretical results suggest that the critical sizes of the nuclei are similar for the various PVDF-based copolymers.

B. P(VDF-BTFE)

As shown in the phase diagram of P(VDF-HFP) in Fig. 3(a), only concentrations with a non-polar ground state can be used to store energy through reversible, electric-field-induced phase transitions. Comparing to P(VDF-CTFE), P(VDF-HFP) actually has limitations, because of the

narrow range of effective concentrations. The reason to use HFP is that the HFP monomer is much larger than the VDF unit. It expands the distances between PVDF chains, giving more space for the dipoles and thus the chains to rotate in the direction of the applied field. Following the same concept, we consider substitution of chlorine in CTFE by bromine. Bromine has similar chemical properties but a significantly larger atomic radius.
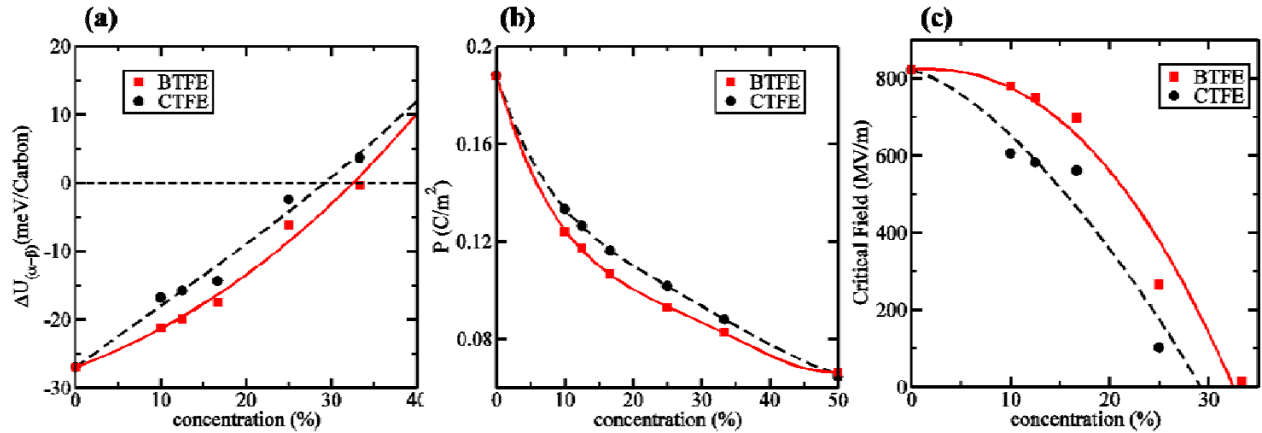
FIG. 5. Phase equilibria and dielectric properties of P(VDF-BTFE) (red) and P(VDF-CTFE) (black) vs. co-monomer concentration: (a) Energy difference between α and β phases (negative value means that the α phase is more stable), (b) Polarization. (c) Critical field at the phase transition.

P(VDF-BTFE) copolymers with varying BTFE concentrations are studied following the same strategy, and phase equilibria and dielectric properties are plotted in Figure 5, with P(VDF-CTFE) used as a benchmark. In contrast to P(VDF-HFP), the energy difference curve of P(VDF-BTFE) is below P(VDF-CTFE). The flipping of the relative stability between non-polar and polar phases occurs significantly later for P(VDF-BTFE) than for P(VDF-CTFE). We thus have a wider choice of co-monomer concentrations in P(VDF-BTFE), because copolymers whose non-polar phase stable at zero electric field have the potential to store energy through the phase transition

16

mechanism. Having a larger bromine atom, the BTFE monomer expands the volume of the copolymer more than CTFE does. It thus makes the polarization per unit volume slightly smaller than in P(VDF-CTFE) at the same monomer concentration. With a larger energy difference between phases and a lower polarization, the calculated critical field is larger for P(VDF-BTFE) than for P(VDF-CTFE) at the same concentration.
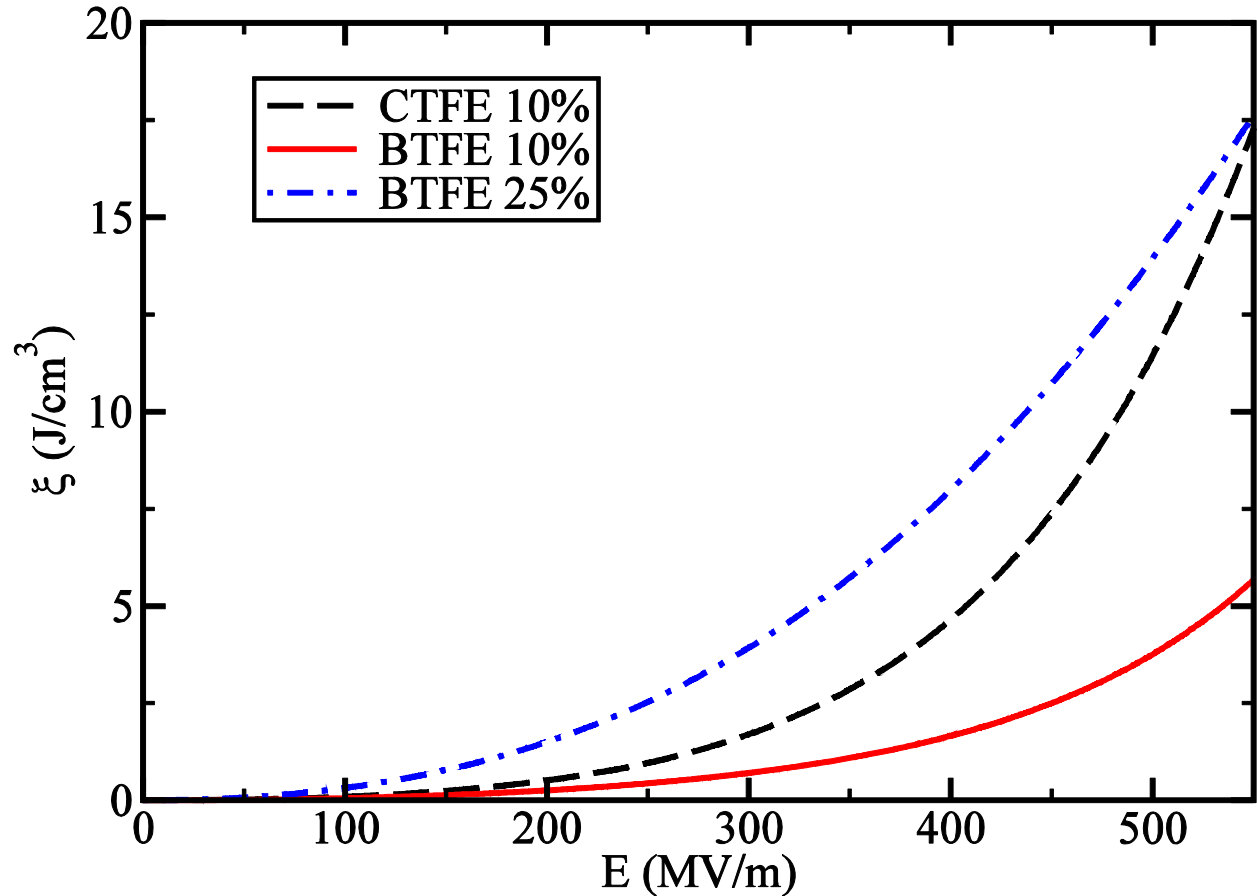
FIG. 6. Energy density as a function of the electric field of P(VDF-BTFE) 10% and 25%, and 10% P(VDF-CTFE).The co-monomer distribution is a Gaussian function with a broadening parameter $\sigma = 8\%$, centered at values showed in the legend. When increasing the concentration from 10% to 25% of BTFE, the low-field performance surpasses that of the benchmark of P(VDF-CTFE) 10%.

The energy densities of P(VDF-BTFE) 10% and 25% are calculated and plotted in Figure 6, with P(VDF-CTFE) 10% used as the benchmark. The broadening parameter of Ref.[6], $\sigma = 8\%$, is also chosen for P(VDF-BTFE). At 10% co-monomer concentration, P(VDF-BTFE) stores less energy than P(VDF-CTFE), because P(VDF-BTFE) requires a larger critical field for transition to the polar phase, i.e., a larger effective onset field. After saturation at about 700 MV/m, the two copolymers have comparable energy densities. Unfortunately, the high field performance is not very important. It is less practical and both the ferroelectric loss and leakage current become significant at high field. To achieve better low field performance, the material needs to be tuned to have a lower critical field. As shown in Figure 5(a), 25% P(VDF-BTFE) has E_c around 300 MV/m. Therefore, it effectively improves energy storage in the low field regime and surpasses P(VDF-CTFE) 10%, see Figure 6.
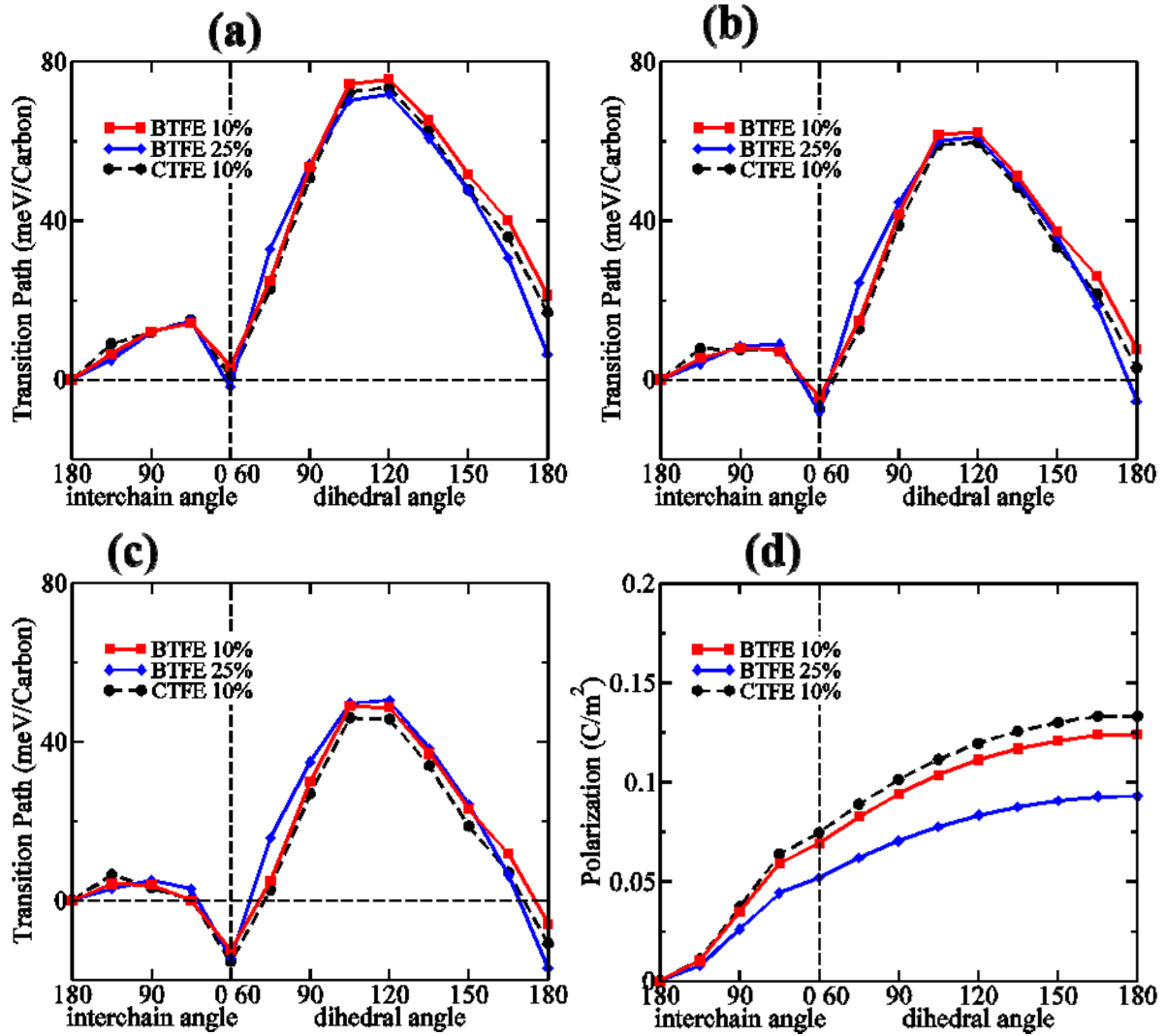
FIG. 7. Total energy along the transition pathway of P(VDF-BTFE) compared with that of P(VDF-CTFE) 10% used as a benchmark: (a) At zero field. (b) At 500 MV/m. (c) At 1000 MV/m. The total energy of the α phase is used as reference and is set to 0. (d) Polarization. The vertical dashed line divides the transition path into two parts, corresponding to the α to γ and γ to β transitions, respectively. The angles are defined in Fig. 2.

The calculated energies and polarizations for the transition pathway are shown for P(VDF-BTFE) 10% and 25%, and for P(VDF-CTFE) 10% in Figure 7. Interestingly, different concentrations of P(VDF-BTFE) have similar barriers in zero electric field (including 33% BTFE, not shown),

which are around 70 meV/carbon atom and very close to the value for P(VDF-CTFE) 10%. This result indicates that these copolymers have very similar dynamical properties. With polarization, the energy barrier is reduced in an electric field, and the reduction is determined by the value of polarization ($\Delta E = -\Omega \vec{P} \cdot \vec{E}$). The enthalpies of intermediate stages with larger polarizations are thus reduced more and a polymer with greater polarization will have a lower barrier at high field. For example, P(VDF-CTFE) 10% has a higher energy barrier than P(VDF-BTFE) in zero electric field, but a lower barrier in 1000 MV/m, see Figure 7. However, this crossover occurs beyond 500 MV/m for P(VDF-BTFE) 10% and 25%, which does not conflict with our previous suggestion that high BTFE concentration P(VDF-BTFE) will have a better low field performance than P(VDF-CTFE) 9% and P(VDF-HFP) 4.5%.

For some copolymer concentrations and electric field values that we considered, the calculated enthalpy of the γ phase is somewhat lower than that of the initial α phase and/or the final β phase. In that case, the field-induced transformation may not occur or terminate at the γ phase, thereby lowering the dielectric energy that may be stored. In practice, the dielectric film consists of nano-crystalline and amorphous domains [3], and thus only specific domains would be affected. The lack of transformation in particular domains may also lead to strained bonds, increasing transformation barriers and potentially leading to losses through thermal stress or generation of electrically active defects. A detailed investigation of loss mechanisms is beyond the scope of this paper.

In general, given that the three copolymers considered here have similar phase diagrams, transformation pathways and barriers, one can consider a mixture of all three to obtain the best properties for specific applications. The considerations should include not only the ultimate energy density at low, practically attainable fields, but also morphology, since a distribution of

crystalline nano domain sizes is necessary for a gradual increase in dielectric displacement needed in applications. Furthermore, imperfections that either pin nano domains or lead to conductive losses must be avoided. Even synthesis of single chains with prescribed composition can be a challenge. For example, current synthesis efforts of P(VDF-BTFE)[23] led to clustering of BTFE, inhibiting crystallization and limiting solubility. Processing considerations in manufacturing large area thin films required for dielectric applications are also important, as is of course cost. Since many of these aspects cannot be predictively simulated at present we refrain from suggesting a specific concentration of monomers, and just point out that that the three co-monomers are predicted to act similarly when mixed with PVDF, thus offering a rich spectrum of possibilities for materials and processing optimization.

IV. SUMMARY AND CONCLUSIONS

In this paper, we investigate via first-principles simulations phase equilibria and transition pathways of two PVDF-based copolymer systems – P(VDF-BTFE) and P(VDF-HFP), and compare them to the previously studied P(VDF-CTFE). We find that the same non-polar to polar phase transition mechanism exists in both copolymers. Furthermore, P(VDF-HFP) 4.17% and P(VDF-CTFE) 10% behave almost identically in all calculated aspects. This result agrees with experiments performed with P(VDF-HFP) 4.5% and P(VDF-CTFE) 9%, which show that these two copolymers have very similar energy density curves. These results confirm that our phase transition model is sufficient to capture the essentials of the high energy density dielectric storage mechanism in this novel class of PVDF-based copolymers.

For the P(VDF-BTFE) copolymer, our results show that it prefers the non-polar phase in a larger range of concentrations than either P(VDF-CTFE) or P(VDF-HFP). It thus offers more freedom to optimize the concentration of the co-monomer for target applications. However, at a

given co-monomer concentration, P(VDF-BTFE) requires a higher critical field than P(VDF-CTFE), making the optimization procedure non-trivial. Nevertheless, we show that P(VDF-BTFE) 25% performs better in the low field regime than P(VDF-CTFE) 10%. In general, the three candidate co-monomers for admixing into PVDF: CTFE, HFP, and BTFE, modify the phase equilibria and transformation properties of PVDF in a similar way, and offer a rich palette for devising P(VDF-copolymer) systems with desired dielectric properties, morphology and processability.

Acknowledgements

[1] B. Chu, X. Zhou, K. Ren, B. Neese, M. Lin, Q. Wang, F. Bauer, and Q.M. Zhang, Science **313**, 334 (2006).

[2] X. Li, X. Qian, S.G. Lu, J. Cheng, Z. Fang, and Q.M. Zhang, Appl. Phys. Lett. **99**, 52907 (2011).

[3] A.J. Lovinger, Science **220**, 1115 (1983).

[4] H. Nalwa, *Ferroelectric Polymers: Chemistry, Physics and Application* (Marcel Dekker, New York, 1995).

[5] H. Su, A. Strachan, and W.A. Goddard, Phys. Rev. B **70**, 64101 (2004).

[6] V. Ranjan, L. Yu, M. Buongiorno Nardelli, and J. Bernholc, Phys. Rev. Lett. **99**, 47801 (2007).

[7] G. Samara, *Solid State Physics* (Academic, San Diego, 2001).

[8] S. Zhang, C. Zou, D.I. Kushner, X. Zhou, R.J. Orchard, N. Zhang, and Q.M. Zhang, IEEE Trans. Dielectr. Electr. Insul. **19**, 1158 (2012).

[9] Q.M. Zhang, V. Bharti, and X. Zhao, Science **280**, 2101 (1998).

[10] L. Yang, X. Li, E. Allahyarov, P.L. Taylor, Q.M. Zhang, and L. Zhu, Polymer **54**, 1709 (2013).

[11] X. Zhou, X. Zhao, Z. Suo, C. Zou, J. Runt, S. Liu, S. Zhang, and Q.M. Zhang, Appl. Phys. Lett. **94**, 162901 (2009).

[12] R. Hasegawa, Y. Takahashi, Y. Chatani, and H. Tadokoro, Polym. J. **3**, 600 (1972).

[13] See Supplemental Material at URL for sample coordinate files.

[14] V. Ranjan, M. Buongiorno Nardelli, and J. Bernholc, Phys. Rev. Lett. **108**, 87802 (2012).

[15] P. Giannozzi, S. Baroni, N. Bonini, M. Calandra, R. Car, C. Cavazzoni, D. Ceresoli, G.L. Chiarotti, M. Cococcioni, I. Dabo, and others, J. Phys. Condens. Matter **21**, 395502 (2009).

[16] D. Vanderbilt, Phys. Rev. B **41**, 7892 (1990).

[17] H.J. Monkhorst and J.D. Pack, Phys. Rev. B **13**, 5188 (1976).

[18] T. Thonhauser, V.R. Cooper, S. Li, A. Puzder, P. Hyldgaard, and D.C. Langreth, Phys. Rev. B **76**, 125112 (2007).

[19] S. Grimme, J. Antony, S. Ehrlich, and H. Krieg, J. Chem. Phys. **132**, 154104 (2010).

[20] J.P. Perdew, K. Burke, and M. Ernzerhof, Phys. Rev. Lett. **77**, 3865 (1996).

[21] R. Fletcher, *Practical Method of Optimization* (John Wiley and Sons, New York, 1980).

[22] R.D. King-Smith and D. Vanderbilt, Phys. Rev. B **47**, 1651 (1993).

[23] M.R. Gadinski, C. Chanthad, K. Han, L. Dong, and Q. Wang, Polym Chem **5**, 5957 (2014).